JOURNAL OF PROPULSION AND POWER
Vol. 22, No. 1, January–February 2006

# Ion Detachment in the Helicon Double-Layer Thruster Exhaust Beam

Fernando N. Gesto,* Boyd D. Blackwell,† Christine Charles,‡ and Rod W. Boswell§
*Australian National University, Acton, Australian Capital Territory 0200, Australia*

**This study is devoted to simulating the orbits of the ions in the supersonic beam observed experimentally in the laboratory development of the helicon double-layer thruster. Given the cylindrical symmetry of the problem, the particle orbits are generated in cylindrical coordinates $(r, \phi, z)$, thereby enabling the analysis of magnetic detachment (in which the particles free themselves from the magnetic field of the source) to be confined to the analysis of the curvature of trajectories on the $(r, z)$ plane. Because the trajectory of a magnetized particle in space is helical, detachment can be established if the curvature of $r(z)$ on the $(r, z)$ plane asymptotically approaches zero. The simulation shows that the *detachment surface* is a paraboloid opening in the direction of the expanding magnetic field, with its base along the radial $(r)$ axis oscillating around the axial value $z \approx 0.38$ m. The radius of the ion-beam detachment surface is in agreement with laboratory measurements of the beam density profile in the detachment region.**

## Nomenclature

| | | |
|---|---|---|
| $\boldsymbol{B}$ | = | magnetic field |
| $B_r$ | = | radial magnetic field |
| $B_z$ | = | axial magnetic field |
| $B_\phi$ | = | azimuthal magnetic field |
| $\hat{B}$ | = | unit vector along the magnetic field |
| $i$ | = | index of initial radial coordinate |
| $\boldsymbol{p}(s)$ | = | magnetic-field line trajectory |
| $r$ | = | radial coordinate |
| $r_i$ | = | initial radial coordinate of ion orbit |
| $s$ | = | distance along a magnetic-field line |
| $v_\parallel$ | = | velocity parallel to the magnetic field |
| $v_\perp$ | = | velocity perpendicular to the magnetic field |
| $z$ | = | axial coordinate |
| $\phi$ | = | azimuthal coordinate |

## I. Introduction

LABORATORY experiments have recently shown that current-free electric double layers can be spontaneously created in helicon plasmas expanding in a diverging magnetic field.[1–3] It was suggested that the ion beam measured downstream of the double layer could be used as a source of thrust in a new type of magnetoplasma space thruster presently defined as the helicon double-layer thruster (HDLT).[1] Another type of magnetoplasma thruster is the variable specific impulse magnetoplasma rocket (VASIMR).[4–6]

Detachment of the plasma in the beam exhaust from the magnetic field produced by a magnetoplasma rocket is an element of thrust-vector analysis that involves experimental, analytic, and computational studies. The thrust in the HDLT prototype is generated by an ion beam that exits the nozzle of the thruster at supersonic velocity.[7] The ion beam itself is generated by the formation, at the neck of the nozzle, of a current-free double-layer potential,[1] which accelerates the ions generated in the helicon argon plasma.

In the laboratory (see Sec. II) the HDLT is attached to a diffusion chamber that is pumped down to simulate space. The accelerating potential difference is situated 25 cm along the nozzle $(z)$ axis, and with the present experimental setup this thrust mechanism is only observed[1] in a gas pressure range of 0.013 to 0.267 Pa.

The solenoidal magnetic configuration encasing the helicon plasma source in the HDLT creates a "magnetic" nozzle, whose magnetic geometry in part determines the dynamics of the exhaust flow by influencing the orbits of the charged argon ions in the beam. The expanding magnetic field created by the solenoids influences the shape of the ion beam as it expands into space, giving the beam divergence and thereby affecting the net thrust generated by the beam. In the extreme case, where the magnetic-field intensity is high enough, the charged particles exiting the nozzle will be attached to the closed magnetic-field lines and no net thrust will be provided. At the other extreme, the beam velocity field will be determined mainly by the parallel acceleration across the double layer and will have almost no divergence, so thrust will be generated at maximum efficiency.

The aim of this study is to analyze the trajectories of the HDLT exhaust ion particles in the expanding magnetic field created by the solenoids surrounding the plasma source. In particular, the simulation is used to analyze whether the accelerated ions in the laboratory prototype "detach" from the magnetic field to provide thrust and what influence the magnetic-field strength has on the detachment process. The simulation is particularly important for the understanding of the behavior of the beam exhaust at distances from the nozzle that currently exceed the axial-length scale of the laboratory experiment.

We introduce a new geometric approach to analyzing the magnetic detachment of the ion beam. Traces of the magnetic field and particle trajectories, for different initial radial values $r_i$ across the beam's radial cross section at the *beam origin*, are generated in cylindrical coordinates and traced onto the $(r, z)$ plane. From the particle trajectory traces, the curvature of the orbits $r_i(z)$ is calculated. We then analyze 1) whether the ion motion detaches from the influence of the magnetic field and 2) at what point in its trajectory it detaches.

A charged particle is unmagnetized, or *detached*, if its trajectory has zero curvature. Given that the curvature of motion of a charged particle in a magnetic field may asymptotically approach

Received 12 October 2004; revision received 18 May 2005; accepted for publication 18 May 2005. 

*Graduate Research Student, Plasma Research Laboratory, Research School of Physical Sciences and Engineering; currently at School of Aerospace and Mechanical Engineering, University College, Australian Defence Force Academy, Australian Capital Territory 2600; fernando.gesto@adfa.edu.au.

†Senior Fellow, Plasma Research Laboratory, Research School of Physical Sciences and Engineering, H-1 NF National Plasma Fusion Facility.

‡Senior Research Fellow, Plasma Research Laboratory, Research School of Physical Sciences and Engineering, Space Plasma and Plasma Processing Group.

§Professor, Plasma Research Laboratory, Research School of Physical Sciences and Engineering, Space Plasma and Plasma Processing Group.

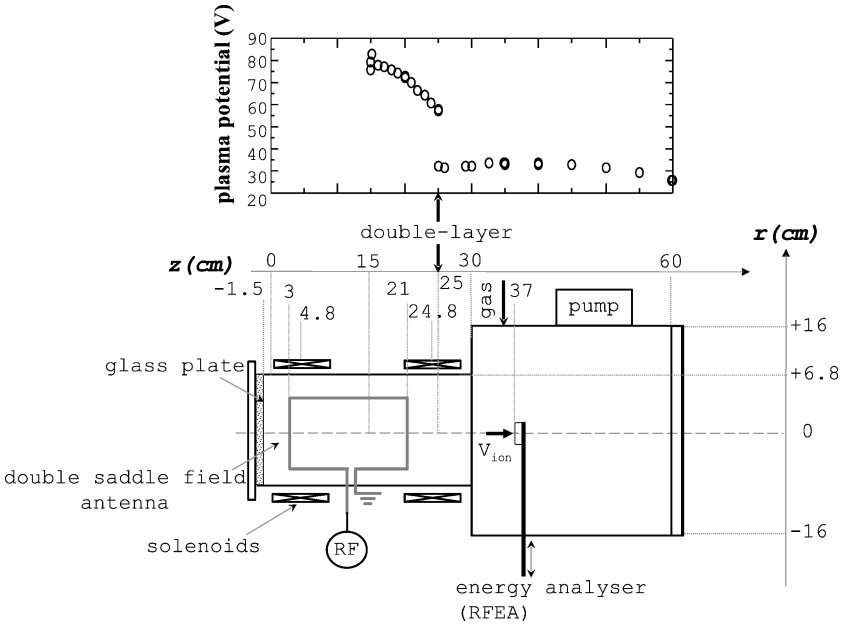


**Fig. 1 Schematic of the HDLT showing the major components of the prototype and the axial location of the double layer at $z = 0.25$ m.**

zero, but theoretically never equal zero, the detachment point is arbitrary. The *order* of the analysis, however, is linear. Detachment (point 1) must be established (curvature approaches zero) before any spatial interpretation (point 2) of detachment can be made. In this paper we seek to establish the point of transition where ion orbits go from a magnetized gyromotion to an unmagnetized near-linear motion. We first establish detachment for single-particle trajectories and then use the cylindrical symmetry of the problem to generate the detachment flux surface of the exhaust beam, as discussed in Sec. IV.

The beam origin is defined at the position of the experimentally measured current-free double layer,[1,7] which accelerates the ions and generates the beam. The initial radial ($r_i$) and axial ($z$) coordinates of the beam origin are $(r, z) = (r_i, 25\text{ cm})$. The maximum initial radius of the ion beam, determined by the internal radius of the plasma source tube within the nozzle, is $r_i = 6.7$ cm. The position of the double layer and internal radius of the nozzle are presented graphically in Fig. 1.

An introduction to the experimental setup of the HDLT is given in Sec. II. The code and the parameters used in the simulation are outlined in Sec. III. Section IV presents and discusses the results of this detachment analysis, and Sec. V concludes with the possible directions in which this first analysis may proceed.

### A. Previous Studies of Detachment

The process of plasma detachment from a magnetic nozzle has been previously studied theoretically[8,9] and by computer simulation.[6,8,10] In this initial work we investigate only the ions, as the momentum carried by the ion beam provides the main source of thrust and is directly measurable in the laboratory experiment. This analysis is therefore in the spirit of the VASIMR,[10] where a particle-trajectory method is used to describe the dynamics of the VASIMR exhaust.

In reality, the faster transport of electrons along field lines because of their smaller mass will set up an ambipolar electric field that will allow the high-energy tail of the electron distribution to drift toward the ions.[11] This feedback is not incorporated into our model, and we recognize that the ambipolar detachment considered in previous studies[6,8,10] is distinct from the orbital detachment considered in this initial work.

Because we treat only the ions in this initial study, we briefly discuss our view on the neglect of ambipolar diffusion in our model.

### B. Particle Detachment and Ambipolar Diffusion

The inclusion of a self-consistent electric field is one of the most challenging problems in current research on plasma simulation. To our knowledge, it has only been achieved in special cases, in which simplifying assumptions could be made, or by heuristic and/or iterative methods.

The problems associated with the magnetic detachment and confinement of plasma flows are attracting a considerable research effort, and, in the case of magnetic detachment, progress is being made experimentally and numerically with particle codes such as the one presented in this paper and codes such as those mentioned previously in Sec. I.A. However, the neutralization of the ion beam by electrons cannot be simply explained by linear fluid or particle dynamics. This problem is related to anomalous cross-field heat flux carried by electrons, which is also an active area of research.

In our case, the simulation has been guided by experiment, where we have measured a very low divergence of the ion beam downstream of the electric double layer. This suggests that the ion beam is well neutralized and that a transport mechanism exists that allows the electrons to follow the ions. Experimentally (see Sec. II) there is evidence that there are sufficient energetic electrons to overcome the potential barrier of the double layer and the beam will be neutral. Hence, in the HDLT, as in all magnetoplasma rockets, there is no need for a hollow cathode neutralizer.

Currently we do not believe that the electron motion will change the trajectories of the ions substantially, although we acknowledge that quantitative proof of this will have to wait for some time. Notwithstanding this caveat, the simulated results discussed in Sec. IV are in good agreement with the laboratory measurements of the ion-beam geometry given by the beam density profile in the detachment region. The results presented in this study therefore provide an *initial understanding* of the HDLT thrust vector.

Thus, the aim of this paper is to complement the current research being undertaken in the electric-propulsion community and to set the platform for more sophisticated future studies of the HDLT.

## II. Laboratory Experiment

The HDLT, represented graphically in Fig. 1, is a horizontal helicon system, consisting of a helicon plasma source. The source is a 32-cm-long glass tube of internal radius $r = 6.8$ cm,

surrounded by a double-saddle antenna that is fed from a rf-matching network/generator system operating at 13.56 MHz. The source is attached contiguously to an aluminium diffusion chamber 30 cm in length and 16.8 cm in radius. The argon feed gas and the turbomolecular/rotary pumping system are connected to the sidewall of the chamber. The base pressure is $2.7 \times 10^{-4}$ Pa, measured with an ion gauge and a baratron gauge, both attached to the diffusion chamber. Tests performed with the gas injection at the closed end of the source tube showed similar results for the present experimental conditions. The present operating pressure conditions correspond to a molecular-flow regime with a very small pressure gradient within the system.

Two solenoids encircling the source and centered at approximately $z = 4.8$ cm and $z = 24.8$ cm create an expanding magnetic field from inside the source into the chamber. Previous laboratory experiments on the HDLT (Refs. 1 and 7) have quoted a current of 6 A through each of the magnetic-field coils and a subsequent calculated axial magnetic field $B_z$ of 250 G in the source. Recent inspection has shown that each magnetic coil comprises two separate windings in parallel, resulting in only 3 A passing through each winding. Consequently the field claimed in these previous publications has been overestimated by a factor of two. In this study we analyze ion orbits in the correct field to ascertain whether detachment is likely to take place in the actual experimental setup. The calculated $B$ field has been checked using a gaussmeter.

Current-free electric double layers have been diagnosed in a number of experimental devices worldwide, all based on the helicon technology.[1–3] This type of double layer spontaneously forms in low-pressure plasmas (below 1 Pa) created in a helicon source with insulating walls and expanding in a physical and magnetic nozzle.

For the present study the rf power, magnetic field, and pressure conditions are set at 250 W, 120 G, and 0.04 Pa, respectively. It has been previously shown[7] that for these experimental parameters, an electric double-layer is generated 25 cm into the source tube, a position close to the physical (geometric expansion due to the change of diameter) and magnetic nozzle (Fig. 1).

The potential drop of the double layer, which generates the ion beam, is measured by a retarding field energy analyzer (RFEA) and is approximately 25 eV. The double layer in the HDLT accelerates the ions that provide the thrust and the ion beam is also characterized using the RFEA.

The RFEA has been described in detail.[12] In brief, it consists of four grids (a grounded grid, a repeller, a discriminator, and a secondary) and a collector separated by insulators and encased in a $3.6 \times 1.9 \times 1.0$-cm grounded metal casing attached to a supporting tube and inserted through a port on the diffusion chamber (Fig. 1). The analyzer aperture is 0.5 mm in diameter.

The RFEA is connected to a LABVIEW data-acquisition system to collect the current vs discriminator voltage characteristic from which plasma parameters such as the plasma density and the ion-beam energy can be measured. For the present conditions, the energy resolution[12] is 1 eV.

The experimental uncertainty in the plasma potential and ion-flux measurements are about 1 V and 15%, respectively. The double layer spontaneously forms during plasma breakdown and is stable thereafter.[7] Although it can be maintained for an hour or more, the time necessary for acquiring a RFEA characteristic is about 20 s.

The double layer and the corresponding ion-beam characterization have shown that there are sufficient energetic electrons to overcome the potential barrier of the double layer, because its strength is about three times the downstream electron temperature,[1] that is, less than a wall sheath potential in argon.[13] Hence, the beam will be neutral.

We were not able to experimentally observe the double layer (or the accelerated ion beam) for pressures greater than about 0.267 Pa. The ion beam will be degraded as the pressure increases because of the increasing frequency of ion-neutral collisions (charge exchange and elastic collisions). At 0.040 Pa, the pressure in the present laboratory experiment, the mean free path is approximately 12 cm whereas the results of the simulation in Sec. IV show that detachment of the ions from the influence of the magnetic field occurs at approximately 13 cm downstream of the double layer. Therefore, for most of the ion motion before detachment, the trajectory will be collisionless.

The configuration of the HDLT leads to a magnetic-field-*aligned* electric field that can be sustained for pressures around 0.04 Pa, for rf powers up to 1 kW or more and for a minimum magnetic field of about 60 G. The internal radii of the source tube (where the plasma is created) and the diffusion chamber (where the ion beam is directed and its measurements taken) are $r = 6.8$ cm and $r = 16$ cm, respectively. The *main* parameters integrated into the simulation of the ion orbits are the current in the solenoids (3 A) and the potential drop of the double layer or the ion-beam energy (25 eV). The numerical simulation is discussed in the next section.

## III. Simulation

Because the problem is essentially the inverse of charged-particle confinement, the HELIAC code, originally developed for optimizing magnetic confinement geometries for plasmas, is adapted to reflect the magnetic configuration of the prototype and used to simulate the *actual* charged-particle trajectories (not the guiding centers) in the laboratory exhaust beam. For circular filamentary coils the magnetic field at a given position is determined by the equations

$$B_r = \left(\frac{I\mu}{\pi}\right)\left(\frac{a}{r}\right)^{\frac{1}{2}}\left(\frac{zk}{4ar}\right)\left[-K + \frac{2-k^2}{2(1-k^2)}E\right] \tag{1}$$

$$B_z = \left(\frac{I\mu}{\pi}\right)\left(\frac{a}{r}\right)^{\frac{1}{2}}\left(\frac{k}{4ar}\right)\left[K + \frac{k^2(a+r)-2r}{2(1-k^2)}E\right] \tag{2}$$

$$B_\phi = 0 \tag{3}$$

where $\mu$ is the magnetic permeability, $I$ is the current in Ampére-turns through the coil, $a$ is the radius of the coil, $r$ and $z$ are the separation between the designated position ($\boldsymbol{r}$) and the center of the coil ($z$), $E$ and $K$ are the complete elliptic integrals,[14] and

$$k^2 = 4ar/[(a+r)^2 + z^2]$$

The trajectory of a magnetic field line $\boldsymbol{p}(s)$ is given by integrating the direction $\hat{B}$ of the magnetic field

$$d\boldsymbol{p}(s)/ds = \hat{B}\,[\boldsymbol{p}(s)] \tag{4}$$

where $\boldsymbol{B}(\boldsymbol{x})$ is the magnetic field at position $\boldsymbol{x}$ and $s$ is the distance along the field line. A modified[15] Adams–Bashforth predictor–corrector algorithm is used with a step size much smaller (<1%) than the minimum radius of curvature of the field line. The HELIAC code was validated by comparison with the analytic forms for straight and circular filaments (on axis) and by comparison with the GOURDON code.[16] Using REAL*8 precision, overall numerical accuracy better than $10^{-8}$ in relative magnetic field and $10^{-6}$ m in traced coordinates was confirmed by comparing two 41-circular-coil models, one composed of circular filaments, the other composed of 5000 finite straight filaments approximating those circular coils.

The equation of motion for a particle with charge $q$ moving in an electromagnetic ($\boldsymbol{E}$, $\boldsymbol{B}$) field is

$$d\boldsymbol{v}/dt = (q/m)[\boldsymbol{E} + (\boldsymbol{v} \times \boldsymbol{B})]$$

Because the electric field $\boldsymbol{E}$ downstream of the double layer is negligible compared to the double-layer potential difference, we simplify the problem by making $\boldsymbol{E} = 0$ and ignoring the ambipolar electric field generated by the different transport rates between electrons and ions. The ion trajectory is then tracked stepwise by integrating the equation of motion:

$$d\boldsymbol{v}/dt = (q/m)[\boldsymbol{v} \times \boldsymbol{B}(\boldsymbol{r})], \qquad d\boldsymbol{r}/dt = \boldsymbol{v} \tag{5}$$

The same integration method was used as for field lines but with time as the independent variable. Choice of step size much

smaller than the gyroperiod ($<1\%$ : $typically$ $<0.01\%$) ensured freedom from numerical instability arising from the implicit nature of these equations and accuracy of the orbit path of $10^{-5}$ m. The code was validated by tracing the precessing orbit of an electron trapped in a dipole magnetic field and confirming conservation of kinetic energy and magnetic moment. Convergence studies, for various step sizes ($\delta s$), confirmed the accuracy of both orbit and field line tracing, and that the convergence was of order $(\delta s)^4$ or better.

Because the double layer that accelerates the ions occurs near the axial ($B_z$) magnetic field maximum,[7] the electric field will be approximately aligned with the magnetic field. The pitch angle of the initial ion velocity to the magnetic-field line will be set at 0 deg to reflect this approximate alignment. Consequently, the initial velocity at the point of acceleration is assumed to be purely axial.

The parameters in the code reflecting the physical configuration of the HDLT are the following:

1) Pitch angle of initial ion acceleration to the magnetic-field line will be 0 deg.

2) Ion mass. The propellant is argon: $m_{\mathrm{Ar}} = 6.63 \times 10^{-26}$ kg.

3) Energy of electric double-layer potential: $E_{\mathrm{dl}} = 25$ eV.

4) Axial position of electric double layer: $z(m) = 0.25$.

5) Radius of the beam at the beam origin: 6.7 cm.

6) Current per coil in solenoid: 3 A.

7) Coil windings per solenoid: $N \approx 720$.

## IV. Results and Discussion

Figure 2 shows the magnetic-field lines and the actual orbits of the exhaust particles generated by the HELIAC code. The helical orbits of the ions in the exhaust beam are projected onto the $(r, z)$ plane. The gyromotion is not pronounced in Fig. 2, and the velocity is mainly axial, because of two features of the HDLT:

1) The acceleration by the double layer $dv_{\parallel}/dt$ is mainly parallel to the magneticfield, and $v_{\perp} \ll v_{\parallel}$.

2) The low magnetic field (120 G).

The axial location and radial cross section of the beam origin, given by the orbits $r_i$, is determined by the experimental diagnostics represented by parameters 4 and 5 of Sec. III. The ion orbits are subject to the Lorentz force, which varies radially. Therefore, the curvature of each orbit will also vary radially and will depend on the orbit starting point $r_i$. This is consistent with the theoretical study of detachment[9] that finds that there are points in space that can be reached from different launching positions $r_i$. Therefore, the ion orbits are defined on the $(r, z)$ plane by their launch positions $r_i$. The curvature of the ion trajectory launched at $r_i = 0.3$ cm is shown in Fig. 3a. The curvature of the ion orbit launched at $r_i = 6.7$ cm is shown in Fig. 3b. The curvature of ions launched at various positions along the beam cross section $(r, z) = (r_i, 0.25)$ m is illustrated in Fig. 4.

It can be seen from Figs. 3 and 4 that the curvature of the orbits reflects the derivative of a sinusoidal segment, which is to be expected because the projection of the helical spatial motion of an ion onto the $(r, z)$ plane is a sinusoidal curve *prior to detachment*. This

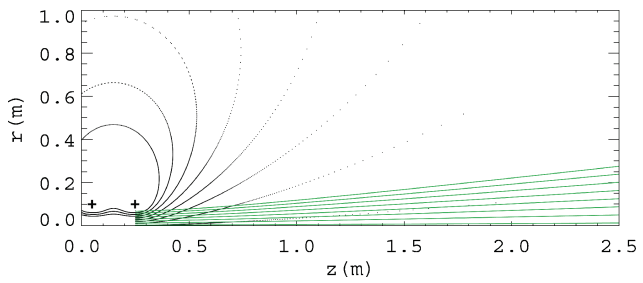


**Fig. 2 Simulated orbits $r_i$ (solid green lines) along argon beam cross section, accelerated by a 25-eV double-layer potential at $(r, z) = (r_i, 0.25)$ m, in a solenoidal magnetic configuration (dotted black lines). The crosses mark the position of the solenoids. The orbits show that the main component of velocity remains axial.**

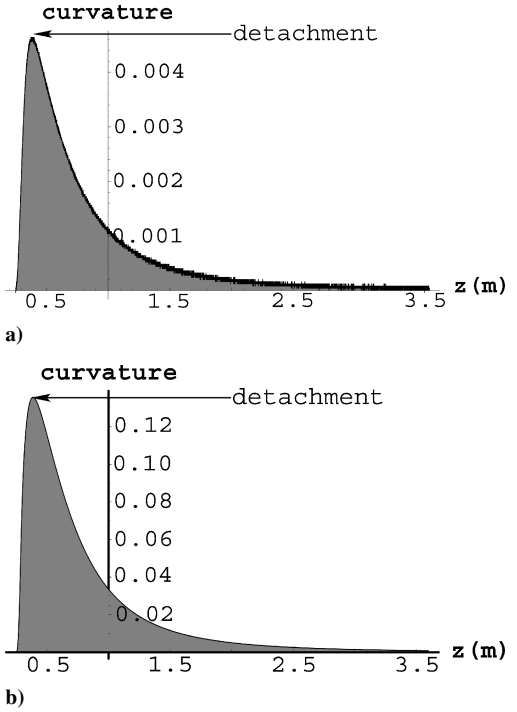


**Fig. 3 Curvature of argon orbits $r_i(z)$ vs $z$: a) curvature of orbit $r_i = 0.3$ cm and b) curvature of orbit $r_i = 6.7$ cm.**

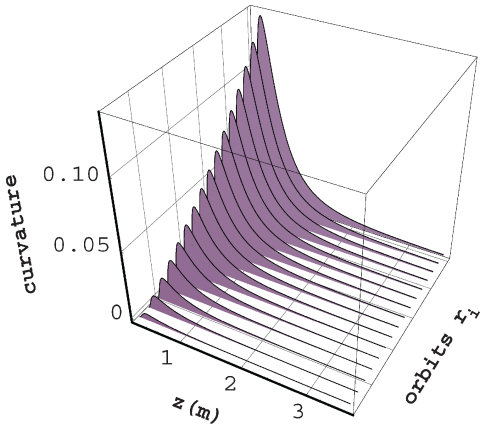


**Fig. 4 Comparison of the curvature of orbits with different launching positions $r_i$.**

postulate will hold given that the simulated orbit does not cross the magnetic axis $z$ and the incremental step size is much smaller than the Larmor radius of the ion orbit being tracked. Figure 4 shows that all the orbits along the entire beam cross section

1) do not complete a single Larmor orbit,

2) increase in curvature toward the beam edge, in the direction of increasing magnetic-field line curvature; and

3) are eventually free, or *detached*, from the magnetic-field influence because the curvature of the projected motion approaches zero. This meets the first condition of the analysis, as set out in Sec. I.

There are two stages in particular that can be identified in the generation of thrust[6] in plasma-propulsion systems. First, the plasma is accelerated out of the nozzle. In the HDLT the acceleration mechanism is a stable potential difference created by the manipulation of experimental parameters. Second, the ions push not only against the vacuum magnetic field as expected but also against the double-layer electric field as they flow essentially linearly out of the nozzle volume. This is the stage where the main thrust is generated. The net thrust generated over time therefore depends upon the reaction force

provided by the electric field of the double layer and the detachment of the flow from the magnetic field and the rocket. Detachment of the ion flow from the closed magnetic field generated by the two solenoids situated around the plasma source is imperative for the propulsion system to generate thrust. Ion flow that remains attached to the magnetic field will return to the flight vehicle, sacrificing momentum gain upon impact.

After we established magnetic detachment, for the purposes of our analysis, the arbitrary *detachment point* for an orbit on the beam cross section in Fig. 2 is defined as the point on the orbit of *maximum* curvature as illustrated in Fig. 3. Past this point, the centrifugal force provided by the magnetic field begins its asymptotic approach to zero, and the Larmor radius of the ions commence diverging from the length scales of the experiment. This is consistent with the particle simulation of plasma detachment in VASIMR,[10] where it is found that the axial ion energy approaches a constant, indicating that the ion motion is not influenced by the magnetic field and that the Larmor radius becomes greater than the radius of curvature of the magnetic field.

Given the cylindrical symmetry of the flow, each curve in Fig. 2 is independent of the angular coordinate $\phi$. This means that each point on the $(r, z)$ plane represents a circular curve in spatial coordinates. Therefore, for each *detachment point* on an orbit $r_i$ in Fig. 2, there will be a corresponding *circular detachment curve* centered at the magnetic $z$ axis. The integral of these curves along $z$ defines the *detachment flux surface* of the ion-beam volume. The detachment flux surface of the ion-beam volume is illustrated in Fig. 5.

The scale of the magnetic $z$ axis in Fig. 5 is exaggerated by a factor of two relative to the radial $r$ axis to highlight the shape of the flux surface. The detachment surface is a "paraboloid" opening in the direction of the expanding magnetic field, with its "vertex" forming a jagged base with discontinuous oscillations around the axial point $z \approx 0.38$ m.

The detachment flux surface on the $(r, z)$ plane is constructed from the detachment points of 23 ion orbits with launch points $r_i$ : $0.001 \leq i \leq 0.67$, along the radial cross section $(r, z) = (r_i, 0.25)$ m. Since the magnetic field is a smooth (analytic) function of position, more launch points would provide a finer cross-sectional grid that would smooth out the jagged oscillations at the base of the paraboloid.

Because the principal aim of this study is to determine whether detachment of the exhaust flow takes place, the finer details of the detachment geometry are left for future analysis. The edge of the paraboloid near the magnetic axis is discontinuous because the Lorentz force is zero at the magnetic axis.

Ions whose velocity vectors are aligned with the magnetic axis detach instantly at the point of acceleration by the double layer.

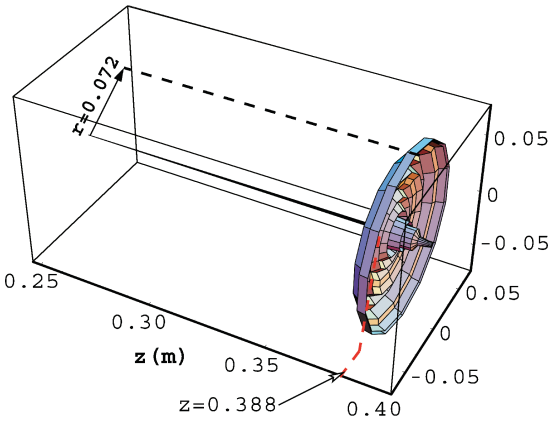


**Fig. 5 Detachment flux surface of the argon exhaust beam. The "paraboloid" has a radius $r = 7.2$ cm. The base is jagged along $r$ and is located on average at $z = 38$ cm. The scale of $z$:$r$ is 2:1 to highlight the shape of the surface. The surface is discontinuous at the magnetic axis.**

In Hooper's theoretical study,[9] detachment of the plasma from the magnetic flux surface, in the field generated by a current loop, is a function of the dimensionless parameter $G$,

$$G = \frac{(eB_z r_0)^2}{4m_e m_i (v_0)^2}$$

where $e$ is the charge, $B_z$ is the axial magnetic-field component, $m_{e,i}$ is the mass of the electrons and ions respectively, $r_0$ is the initial radial coordinate, and $v_0$ is the initial flow velocity. By separating the term $r_0$, we can see that $G$ is proportional to the ratio defined by the square of the initial radial position divided by the product of the electron and ion initial momenta. The Larmor radii in turn are the perpendicular components of these initial flow energies. Defined in these terms, the dynamical process places an interesting constraint on the initial conditions in the geometrical detachment model presented here. Any spatial reorientation of the accelerating double layer from its alignment with the magnetic field will affect the initial pitch angle of the test ions and consequently the initial Larmor radius of the ions. The orientation of the initial acceleration will not change the magnitude of the initial flow energy, as the summation of the perpendicular and parallel velocities must remain constant. Therefore, the ion flow will be within a detachment range for all pitch angles. Because we do not incorporate electron motion in our numerical analysis of detachment, further comparison of the results with Hooper's analytic derivation will be left for the future development of the current model.

The location and shape of the detachment surface, however, will depend on the initial velocity components. As stated in Sec. III, this study assumes that the electric double layer is aligned with the magnetic field because experimentally[7] the location of the double layer is close to the axial magnetic-field maximum. The detachment flux surface inside the ion-beam outer surface is illustrated in Fig. 6. Here the $z$:$r$ ratio is 1:1, illustrating the almost cylindrical geometry of the beam volume and high thrust efficiency at detachment. The angle of divergence of the outer beam surface at the point of detachment is approximately 2.16 deg. The flow near the magnetic axis diverges only 0.04 deg. Because the beam density is greatest at the beam axis, as the experimental density profile in Fig. 7a shows, the propulsion system has high thrust-vector efficiency.

In Fig.7a, the experimental density ratio (open diamonds) of beam ions to background ions across the chamber radius $r$ is obtained with the retarding field energy analyzer located at $z = 37$ cm and facing the double-layer potential on the magnetic $z$ axis.

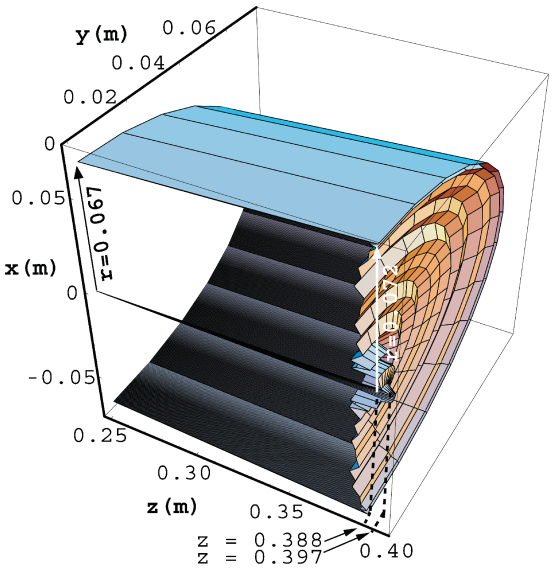


**Fig. 6 Cross section of the argon ion-beam exhaust, showing the detachment flux surface inside the beam volume outline. The radius of the beam increases from 6.7 cm at the point of acceleration by the double layer to 7.2 cm at detachment.**

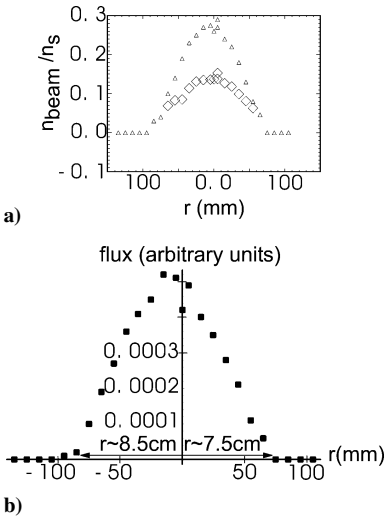


**Fig. 7 Experimental density profile across the chamber radius $r$ at $z = 37$ cm. The experimental flux[7] of beam ions across the nozzle radius $r$ is also measured at $z = 37$ cm: a) experimental density ratio across the nozzle chamber radius and b) experimental flux across the nozzle chamber radius.**

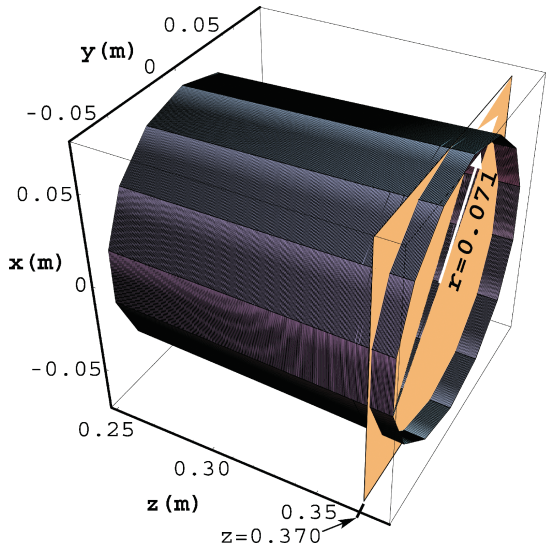


**Fig. 8 Three-dimensional simulation of the argon ion beam showing the radius $r$ of the beam at $z = 37$ cm. The radius of the beam at this axial coordinate is 7.1 cm, which is in agreement with the laboratory measurements (Fig. 7) of the beam's radial profile measured at the same axial position.**

The small triangles correspond to the upper limit for the beam-density ratio derived from the Gaussian fits to the ion-distribution functions.[7]

For the present experimental conditions, the ion-beam density on the $z$ axis derived from the RFEA measurements is $1.5 \times 10^9$ cm$^{-3}$. The experimental uncertainties in Fig. 7a are $\delta(n_{\text{beam}}/n_s) \approx \pm 0.02$ and $\delta(r) \approx \pm 1.0$ mm, whereas the flux uncertainty in Fig. 7b is 15%.

The geometry of the beam is in good agreement with the laboratory measurements[7] represented in Fig. 7b where the energy analyzer measures, at $z = 37$ cm, the flux of "beam" ions with energies equivalent to the double-layer potential difference. This flux is contained within the approximate range $8.5\,\text{cm} < r < 7.5$ cm, which compares well with the radius of the simulated ion beam at this axial location. Figure 8 shows that the radius of the simulated ion beam at $z = 0.37$ m is 0.071 m. Therefore, the *net* uncertainty in the model, because of experimental uncertainty and intrinsic simplifications in the model itself, is of the order of approximately 10%. Notwithstanding experimental uncertainty, the slight difference in radius is consistent with the modeling assumptions, because the ambipolar electric field, which has been neglected in the modeling, will in reality act on the ions and give the beam more divergence. The consistency between the simulated and experimental results suggests that computational analysis of the HDLT thrust vector can proceed with a degree of confidence.

## V. Conclusion

In this initial study we have simulated the supersonic argon-ion beam of the HDLT formed when the ions are accelerated by the potential drop of an electric double layer. The study used a new geometric approach to analyze the influence of the magnetic field on the ion flow and the generation of thrust, and we found the following results:

1) The ion beam detaches from the magnetic field. This is an important result, because nondetachment of all or part of the flow sacrifices all or part of the momentum gained.

2) The simulated flow has a small angle of divergence, which increases radially in the direction of magnetic-field curvature.

3) The geometry of the simulated beam in the detachment region is found to be in agreement with laboratory measurements.

The following areas need to be explored in future studies:

a) The spatial positioning of the double layer. A detailed study of the spatial orientation of the double layer and the subsequent influence of the pitch angle at the point of acceleration on the detachment geometry is an important area for future analysis.

b) The study of electron motion and magnetic detachment.

c) The influence of ambipolarity on the ion beam.

d) The use of other propellants in the source.

The consistency between the simulation and experimental measurements with the propellant argon allows us to confidently proceed with the computational analysis of the exhaust for propellants and parameters that do not have the same detailed laboratory experimentation available for verification.

## References

[1]Charles, C., and Boswell, R. W., "Current-Free Double-Layer Formation in a High-Density Helicon Discharge," *Applied Physics Letters*, Vol. 82, No. 9, March 2003, pp. 1356–1358.

[2]Cohen, S. A., Seifert, N. S., Stange, S., Boivin, R. F., Scime, E. E., and Levington, F. M., "Ion Acceleration in Plasmas Emerging from a Helicon-Heated Magnetic-Mirror Device," *Physics of Plasmas*, Vol. 10, No. 6, June 2003, pp. 2593–2598.

[3]Sun, X., Biloiu, C., Hardin, R., and Scime, E., "Parallel Velocity and Temperature of Argon Ions in an Expanding, Helicon Source Driven Plasma," *Plasma Sources Science and Technology*, Vol. 13, May 2003, pp. 359–370.

[4]Chang Diaz, F. R., "Research Status of the Variable Specific Impulse Magnetoplasma Rocket," *Transactions of Fusion Technology*, Vol. 35, Jan. 1999, pp. 87–93.

[5]Squire, J. P., Chang Diaz, F. R., Baity, F. W., Barber, F. C., Carter, M. D., Goulding, R. H., Sparks, D., McCaskill, G., Ilin, A. V., Bengston, R. D., Bussell, R. G., Jr., Jacobson, V. T., and Glover, T. W., "Experimental Status of the Development of a Variable Specific Impulse Magnetoplasma Rocket," *Transactions of Fusion Technology*, Vol. 35, Jan. 1999, pp. 243–247.

[6]Arefiev, A. V., and Breizman, B. N., "Theoretical Components of the VASIMR Plasma Propulsion Concept," *Physics of Plasmas*, Vol. 11, No. 5, May 2004, pp. 2942–2949.

[7]Charles, C., and Boswell, R. W., "Laboratory Evidence of a Supersonic Ion Beam Generated by a Current-Free Helicon Double-Layer," *Physics of Plasmas*, Vol. 11, No. 4, April 2004, pp. 1706–1714.

[8]Rax, J. M., Haug, C., Chabert, P., and Robiche, J., "Ion Cyclotron Resonance and Electron Cyclotron Resonance Plasma Thrusters," Laboratoire de Physique et Technologie des Plasmas, Ecole Polytechnique, T.R. Estec16217/02/NL/PA, Palaiseau, France, Dec. 2002.

[9]Hooper, E. B., "Plasma Detachment from a Magnetic Nozzle," *Journal of Propulsion and Power*, Vol. 9, No. 5, 1993, pp. 757–763.

[10]Ilin, A.V., Chang Diaz, F. R., Squire, J. P., Tardity, A. G., Breizman, B. N., and Carter, M. D., "Simulations of Plasma Detachment in VASIMR," AIAA Paper 2002-0346, Jan. 2002.

[11]Harvey, R. W., McCoy, M. G., Hsu, J. Y., and Mirin, A. A., "Electron Dynamics Associated with Stochastic Magnetic and Ambipolar Electric Fields," *Physical Review Letters*, Vol. 47, No. 2, 1981, pp. 102–105.

[12]Charles, C., Degeling, A. W., Sheridan, T. E., Harris, J. H., and Lieberman, J. H., "Absolute Measurements and Modeling of Radio Frequency Electric Fields Using a Retarding Field Energy Analyzer," *Physics of Plasmas*, Vol. 7, No. 12, Dec. 2000, pp. 5232–5241.

[13]Lieberman, M. A., and Lichtenberg, A. J. (eds.), *Principles of Plasma Discharges and Materials Processing*, Wiley-Interscience, New York, 1994, Chap. 6, p. 161.

[14]Abramowitz, M., and Stegun, I. (eds.), *Handbook of Mathematical Functions*, Dover, New York, 1965, Chap. 17.

[15]Blackwell, B. D., McMillan, B., Searle, A. C., and Gardner, H. J., "Algorithms for Real-Time Magnetic Field Tracing and Optimisation," *Computer Physics Communications*, Vol. 142, No. 1–3, 2001, pp. 243–247.

[16]Gourdon, C., Marty, D., Mashke, E. K., and Touche, J., "The Torsatron Without Toroidal Field Coils as a Solution of the Divertor Problem," *Nuclear Fusion*, Vol. 11, No. 2, 1971, pp. 161.